

Mode Switch Assistance to Maximize Human Intent Disambiguation

Deepak Gopinath^{*†}, Brenna D. Argall^{*†‡§}

^{*}Department of Mechanical Engineering, Northwestern University, Evanston, IL

[†]Shirley Ryan AbilityLab, Chicago, IL

[‡]Department of Physical Medicine and Rehabilitation, Northwestern University, Chicago, IL

[§]Department of Electrical Engineering and Computer Science, Northwestern University, Evanston, IL

deepakgopinath@u.northwestern.edu

brenna.argall@northwestern.edu

Abstract—In this paper, we develop an algorithm for intent inference via goal disambiguation with a shared-control assistive robotic arm. Assistive systems are often required to infer human intent and this usually becomes a bottleneck for providing assistance quickly and accurately. We introduce the notion of *inverse legibility* in which the human-generated actions are legible enough for the robot to infer the human intent confidently and accurately. The proposed disambiguation paradigm seeks to elicit legible control commands from the human by selecting control modes that *maximally disambiguate* between the various goals in the scene. We present simulation results which look into the robustness of our algorithm and the impact of the choice of confidence functions on the performance of the system. Our simulations results suggest that the choice of confidence functions is a critical factor in determining the disambiguation algorithm’s capability to capture human intent in an intuitive way. We also present a pilot study that explores the efficacy of the algorithm on real hardware with promising preliminary results.

I. INTRODUCTION

Assistive and rehabilitation devices such as powered wheelchairs, robotic arms and myoelectric prostheses play an important role in the lives of people with motor impairments. These devices help to increase their ability to perform activities of daily lives and reduce their dependence on caretakers, and are crucial to revolutionizing the way people with motor impairments interact with society. As the field of assistive robotics progresses rapidly, the devices themselves become more capable and dextrous—and as a result also more complex, higher dimensional and harder to control.

The common paradigms for operating such high-dimensional devices have the human directly control the device motion via a control interface. However, the more severe a person’s motor impairment, the more limited are the control interfaces available for them to use. These interfaces (for example, a switch-based head array or Sip-N-Puff) are lower in dimensionality and bandwidth, and usually require more mode switches for successful task completion. Therefore, we have a difficult situation, in which sophisticated assistive devices that require complex control strategies are paired with users with diminished ability to control them.

Due to the mismatch between the dimensionality of the control interface and controllable degrees-of-freedom (DOF) of the robotic device, control interfaces typically operate in

modes which correspond to different partitions of the control space. By necessity, the more limited the control interface is, the greater number of modes there are. In order to have full control of the robot the user will have to switch between the different partitions and this is known as *mode switching* or *modal control* [22, 19].

It has been established that mode switching is expensive and as a result task performance is degraded. Furthermore, it adds to the cognitive and physical burden as each of these mode switches requires the user to shift their attention from the task to performing the mode switch. The introduction of *shared autonomy* to these systems helps to alleviate and address some of these issues by letting the system take partial responsibility of task execution, thereby reducing the human effort in achieving a goal. For any assistive autonomy, the system typically needs an idea of what it is the human is trying to do—either by explicit indication from the user of the task or goal [6], or by inferring the human’s intent from their control signals and/or sensor data. The question of intent inference is key. In this paper, we develop an assistance paradigm that helps with intent inference, by selecting the control mode in which robot motion will *maximally disambiguate* human intent. The faster the autonomy is able to disambiguate intent, the earlier the robot is able to provide autonomy assistance—leading ideally to fewer mode switches and less burdensome executions.

Within the field of Human-Robot Interaction (HRI) a *legible* motion is one which helps the observer (usually the human) decipher the intent behind the robot’s action more *quickly* and *confidently*. It can be the case that certain actions *by the human* might carry more information about

the human’s intent—which can then help the robot to draw useful and correct inferences more easily. Therefore, in this paper we propose a paradigm of *inverse legibility* in which

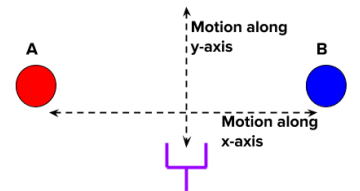


Fig. 1. Illustration of goal disambiguation along various control dimensions. Any motion of the end effector (purple) along the y-axis will not help the system to disambiguate the two goals (A and B). However, motion along the x-axis provides cues as to which goal.

the roles are switched and the human-generated actions *help the robot* to infer human intent confidently and accurately.

Consider the example illustrated in Figure 1. A human control command issued along the x dimension is more *intent expressive* and helps the robot to provide the right kind of assistance quickly and confidently. With the disambiguation assistance scheme developed in this work, we hope to elicit more legible *human* control commands by placing the user control in those modes that *maximally disambiguate* between the various goals in the scene.

In Section II we present an overview of relevant research in the area of shared control in assistance systems focusing on mode switching, legibility and synergies in HRI. Section III describes the mathematical formalism for the algorithm and the metric used for goal disambiguation. The simulation results are presented in Section V, and the pilot study in Section VI. Conclusions are provided in Section VII.

II. RELATED WORKS

This section provides a brief overview of related research in the areas of intent inference, robot assistance for modal control, legibility and cooperation in HRI.

Shared-control assistance paradigms help to offload cognitive and physical burden [23] without requiring the user to relinquish complete control, and are usually preferred over fully autonomous assistive robotic systems for reasons of both robustness and user satisfaction. Often, shared control systems require an estimate of the human’s intent—their intended task, goal or motion, for example. Methods for intent inference have been extensively studied by roboticists and cognitive scientists alike and can be broadly classified into two categories: model-based and heuristic-based [4]. In model-based approaches the agent is typically modeled as a Partially Observable Markov Decision Process (POMDP) that acts according to a policy that maps states to actions. In such settings, intent inference reduces to solving the inverse problem of computing the posterior distribution over mental states conditioned on observed actions (Bayesian Inference) [2, 3]. Heuristic-based approaches instead seek to find direct mappings between some signals—such as low-level motion cues [5] or biological signals [7] and the underlying human intention. Heuristic-based approaches usually are computationally less expensive than model-based approaches. Our approach builds on a heuristic-based intent inference framework. More specifically, we use a *confidence function* as a measure of the robot’s estimate that a particular goal is indeed the user’s intended goal. Confidence functions typically depend on the human control command, autonomous policy, robot pose or goal locations, and often are used to dictate how much control lies with the robot versus with the human in the shared-control system.

The cognitive burden of shifting focus (*task switching*) from the task at hand to mode switches can result in a significant decrease in task performance regardless of the control modality [18]. Researchers have also shown that a significant number of users have found *modal control* and *mode switching* to be slow, difficult and burdensome [14].

Even a simple time-optimal automatic mode switching system can significantly improve user satisfaction while maintaining the quality task performance [14]. Another study [13] found that it is not always the case that users are trying to optimize for time or effort during task execution. Our present system therefore does not make *a priori* assumptions regarding the optimizing principles at work when a user operates a robot.

The legibility and predictability of robot motion *to the human* have been thoroughly investigated [11], and different methods for generating legible robot motion have also been proposed [15]. We apply this concept of legibility however to the *human control* commands, such that the intent expressed in the human command is clear *to the robot*. Our assistance scheme is intended to bring out a more legible intent-expressive control command from the human, by placing the user control in that mode which can provide maximal goal disambiguation and improved legibility.

Eliciting legible commands from the user can also be thought of as an information acquisition problem. Information acquisition in robotic systems have been widely studied, primarily in the context of generating optimal control for mobile robotic sensing systems. A typical approach is to model the problem as an optimal control problem with an associated reward structure that reflects some measure of information gain [1]. The problem of information gathering have also been formulated as maximizing the ergodicity of a robot’s trajectory with respect to an underlying information density map [16, 17] by evaluating the expected value of the Fisher information, which is the amount of information a single measurement reveals at a location.

Also related to our work is the idea of mutual cooperation between humans and robots, and the underlying synergies that are crucial for successful human-robot interaction. In order to overcome the communication bottleneck that exists between robots and people during human-robot interactions, different types of user interfaces have been developed by accounting for the constrained capabilities of the robot [12]. Their work exploits the fact that humans are good at changing communication strategies and compensate for limited communication bandwidth effectively thereby not requiring the robots to perfectly understand natural language interactions. A framework for “*people helping robots helping people*” was developed in which humans provide semantic information and judgments about the environment to the robot which then utilizes them to improve its own capabilities [21]. Researchers have also developed a *symbiotic* human robot interaction scheme which aims to overcome perceptual and cognitive limitations that robots might encounter while still allowing the robots to help humans as well [20]. From the robot’s perspective the key concept behind our algorithm is the idea of “*Help Me, Help You*”—that is, if the human can “help” the robot by providing more legible control commands, then the robot in turn can assist the human more quickly and effectively.

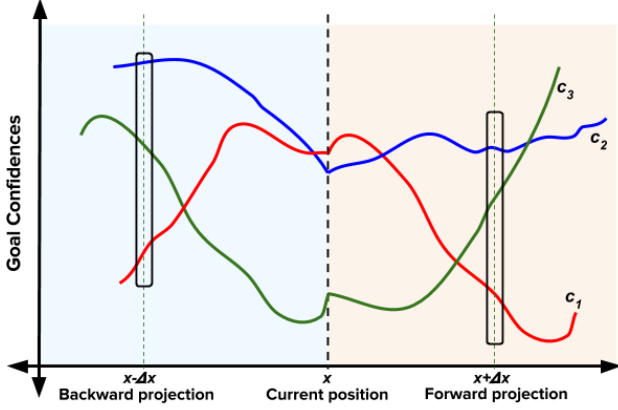


Fig. 2. Illustration of change in confidence with movement along a single control dimension. A very different distribution of confidences results from positive motion (beige) versus negative motion (blue). Snapshots after moving by amount Δx highlighted by rectangles.

III. ALGORITHM DESIGN

This section describes our algorithm that computes the control mode with maximum goal disambiguation, thereby eliciting the most legible control command from the human. Section III-A outlines the mathematical notation used in the paper and Section III-B describes the formulation and computation of the metric used to disambiguate human intent.

A. Notation

Let \mathcal{G} be the set of all candidate user goals with $n_g = |\mathcal{G}|$ and let g^i refer to the i^{th} goal where $i \in [1, 2, \dots, n_g]$. A *goal* represents the intent of the human, and might be a task or location in the world, for example. The set of goals corresponds to an associated set of confidences denoted as \mathcal{C} , where c^i refers to the individual confidence associated with goal g^i —that is, the robot’s confidence that g^i represents the human’s intent. Let \mathcal{K} be the control space in which the robot operates and k^i refer to an individual control dimension where $i \in [1, 2, \dots, n_k]$. The cardinality of \mathcal{K} depends on the robotic platform; for example, for a smart wheelchair $n_k = 2$ whereas for a six degrees-of-freedom robotic arm $n_k = 6$.

For control purposes, the set \mathcal{K} is partitioned into subsets known as *modes*. Let \mathcal{M} refer to the set of all modes that the control space \mathcal{K} is partitioned into with $n_m = |\mathcal{M}|$. The number of modes n_m is specific to the control interface and mapping to \mathcal{K} . Furthermore, let m^i refer to the i^{th} mode where $i \in [1, 2, \dots, n_m]$.

Another quantity of interest is the spatial gradient of individual goal confidences for motions along the various control dimensions. More specifically, the gradient will be denoted by $\frac{\partial c}{\partial x_k}$, where $c \in \mathcal{C}$ and x_k is the component of robot’s position along control dimension k . Furthermore, since the confidence function, in general, can assume drastically different values upon moving in positive and negative directions within a given control dimension, the positive and negative gradients

are explicitly denoted as $\frac{\partial c}{\partial x_k}^+$ and $\frac{\partial c}{\partial x_k}^-$ respectively. The formalism developed in Section III-B is agnostic to the particular form of confidence function. Additionally, an analytical closed-form expression for the gradient might not always be available, as confidence functions need not be continuous and differentiable. Even when available, such an expression might be expensive to compute. In such cases, the gradient can be numerically approximated which we derive in Section III-B4.

We define a *disambiguation* metric $D_k \in \mathbb{R}$ for each control dimension $k \in \mathcal{K}$, which is a function of c and $\frac{\partial c}{\partial x_k}$. Analogous to the gradients, we explicitly define disambiguation metrics for both positive and negative motion directions as D_k^+ and D_k^- respectively. We further define a disambiguation metric $D_m \in \mathbb{R}$ for each control mode $m \in \mathcal{M}$. The disambiguation metric D_m is a measure of how legible the user commands would be if the user were to control the robot in mode m . The higher the value, the easier it will be for the system to infer the human’s intent.¹

B. Disambiguation Metric

The disambiguation metric D_k encodes different aspects of how the goal confidences change upon moving along control dimension k . Figure 2 is an illustrative example which shows how goal confidences can vary as a function of position along a control dimension.

A proper design of D_k should take into account both immediate as well as long term benefits of moving in k . In order to compute the goal confidences after a small user-initiated robot motion we sample the confidence function in the neighborhood $x \pm \Delta x$ of the current pose x of the robot, where Δx is a small change along the control dimension.

If the confidence function depends on the user control command (u_h) then during the sampling procedure the value of u_h is set as $\frac{\Delta x}{\Delta t}$ —that is, the velocity that would result in movement from x to $x + \Delta x$ in one execution timestep Δt .

We identify four important components to inform the design of D_k .

1) *Maximum of confidences*: The maximum of the goal confidences is a good measure of the system’s overall certainty in accurately estimating human intent. A higher maximum implies that the robot has an even better idea of what the human is trying to do. The $\max(\Gamma_k)$ is computed as

$$\Gamma_k = \max_{1 \leq i \leq n_g} c_{\delta_x}^i$$

2) *Difference between largest confidences*: Since it is possible to have multiple² highly confident goals, accurate disambiguation also benefits from a large separation between the first and second most confident goals. This difference is denoted by Ω_k and is computed as

$$\Omega_k = \max(\mathcal{C}_k) - \max(\mathcal{C}_k \setminus \max(\mathcal{C}_k))$$

where \mathcal{C}_k is the set of projections of all goals confidences along control dimension k .

¹Going forward, subscript k will be dropped from x_k for notational brevity.

²Note that confidences are not normalized, since we do care about more than just their relative magnitudes (bullet 2).

3) *Separation in confidences*: A good measure for evaluating the disambiguation potential of a control dimension is to compute the *separation*, Λ_k , in goal confidences. At any point in space this can be computed as the *sum of pairwise distances* between the n_g confidences. Thus,

$$\Lambda_k = \sum_{p=1}^{n_g} \sum_{q=p}^{n_g} |c_{\delta_x}^p - c_{\delta_x}^q|$$

where δ_x indicates $x + \Delta x$ or $x - \Delta x$ depending on the direction of perturbation and $|\cdot|$ denotes the absolute value.

4) *Gradients*: The propensity for change and information gain upon the continuation of motion along control dimension k is encoded in the gradients $\frac{\partial c}{\partial x}$. The greater the difference between the gradients of individual confidences c , the greater will they deviate from each other over time. Instead of using closed-form analytical gradients, we approximate the gradients using forward and backward differences. Therefore,

$$\frac{\partial c}{\partial x} \approx c_{\delta_x} - c_x$$

where c_x denotes the confidence at location x . In order to quantify the “spread” of gradients we define a quantity Υ_k which is computed as

$$\Upsilon_k = \sum_{p=1}^{n_g} \sum_{q=p}^{n_g} \left| \frac{\partial c^p}{\partial x} - \frac{\partial c^q}{\partial x} \right|$$

Putting it all together: Γ_k , Ω_k , Λ_k and Υ_k are then combined to compute D_k as

$$D_k = \underbrace{w \cdot (\Gamma_k \cdot \Omega_k \cdot \Lambda_k)}_{\text{short term}} + \underbrace{(1 - w) \cdot \Upsilon_k}_{\text{long term}} \quad (1)$$

where w controls the relative contribution of immediate and the long term benefit and is task-specific. Equation 1 actually is computed twice, once in each of the positive ($\delta_x = x + \Delta x$) and negative directions ($\delta_x = x - \Delta x$), and the results are then summed. Once the disambiguation metric D_k for each control dimension k is computed, the disambiguation metric D_m for control mode m is calculated as

$$D_m = \sum_k D_k \quad \forall k \in m$$

Lastly, the control mode with highest disambiguation capability m^* is given by

$$m^* = \operatorname{argmax}_m D_m$$

and the control dimension with highest disambiguation capability k^* is given by

$$k^* = \operatorname{argmax}_k D_k$$

Disambiguation mode m^* is the mode that the algorithm chooses *for* the human to better estimate their intent. Any subsequent control command issued by the user in m^* is likely to be more legible due to maximal goal confidence disambiguation.

IV. IMPLEMENTATION

This section describes the details of our implementation. Section IV-A discusses various confidence functions used to infer user intent, followed by the details of the underlying shared control system in Section IV-B.

A. Confidence Function

The algorithm proposed in this paper requires that the confidence measures varies as a function of x , so that $\frac{\partial c}{\partial x}$ is well-defined and exists. The choice of confidence function is up to the system designer and numerous options exist.

We implement two confidence functions in this work. A simple proximity-based confidence function used extensively in the literature [8, 9, 10] is

$$\mathbf{C1}: c(x, x_g) = \max(0, 1 - \frac{\|x - x_g\|}{R})$$

where x is the current position of the robot, x_g is the location of goal g , R is the radius of a sphere beyond which the confidence is always 0 and $\|\cdot\|$ is the Euclidean norm. We refer to this confidence function as **C1**. However, this confidence measure ignores all cues regarding human intent present in the control command itself. A confidence function that aims to capture the “directedness” of the human control command towards a goal contains more information content. One option is

$$\mathbf{C2}: c(x, x_g, u_h) = u_h \cdot (x_g - x)$$

where u_h is the human control command. We refer to this confidence function as **C2**.

B. Control Sharing Paradigm

In our implementation, the proposed disambiguation assistance paradigm augments a blending-based shared control system, in which the final control command issued to the robot is a blended sum of the human control command and an autonomous robot policy. The control signal from

the robot autonomy is generated by a function $f_r(\cdot) \in \mathcal{F}_r$,

$$u_r \leftarrow f_r(x)$$

where \mathcal{F}_r is the set of all control behaviors corresponding to different tasks. Specifically, let $u_{r,g}$ be the autonomous control policy associated with goal g . The final control command u , issued to the robot is then given as

$$u = \alpha \cdot u_{r,g^*} + (1 - \alpha) \cdot u_h$$

where g^* is the most confident goal. The blending factor α is a function of the system’s confidence (Figure 3).

The robot control command $u_{r,g}$ is generated using a simple potential field based dynamical system which is defined in all parts of the state space. In our implementation, each goal is a position in space (x_g). Every goal g is associated with a potential field P_g which treats g as an attractor and all the

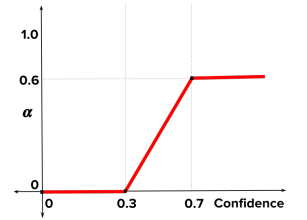


Fig. 3. A prototypical arbitration function.

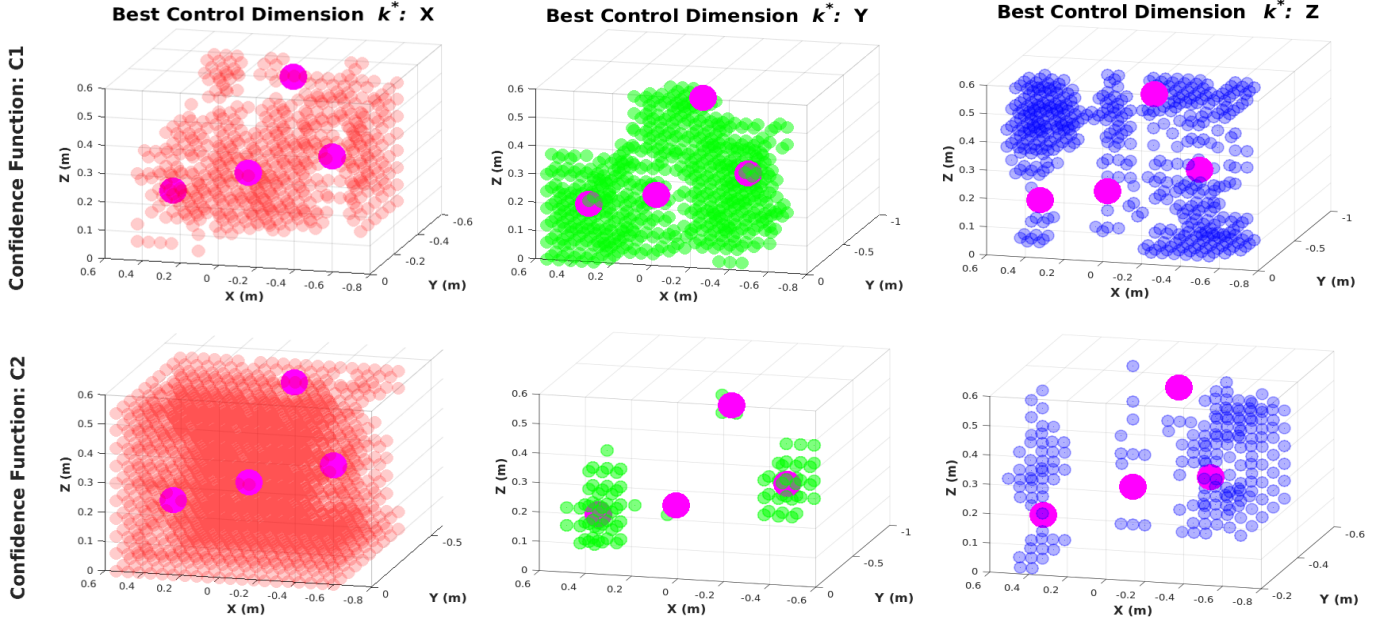


Fig. 4. Control dimensions best able to disambiguate intent. Using confidence functions **C1** (top row) and **C2** (bottom row). Left column: k^* is X. Middle Column: k^* is Y. Right Column: k^* is Z. Magenta spheres indicate the goal locations (intent).

other goals in the scene as repellers. For potential field P_g , the attractor velocity is given by

$$\dot{x}_{attract} = x_g - x$$

where x_g is the location of g . The repeller velocity is given by

$$\dot{x}_{repel} = \sum_{i \in \mathcal{G} \setminus g} \frac{x - x_i}{\eta(\|x - x_i\|^2)}$$

where \dot{x} indicates the velocity of the robot in the world frame and η controls the magnitude of the repeller velocity. Therefore,

$$u_{r,g} = \dot{x}_{attract} + \dot{x}_{repel}$$

Additionally, P_g operates in the full six dimensional Cartesian space and treats position and orientation as independent potential fields.

V. SIMULATION STUDY

In this section we present evaluations of the disambiguation system for correctness within a simulated environment.

A. Choice of Confidence Functions

The choice of confidence functions can greatly affect the computation of k^* and m^* . In order to quantify the disambiguating power of different choices of confidence function, we performed simulations in which k^* was computed at 2000 uniformly sampled points in the workspace of the robot, approximated as a $1.2 \times 0.6 \times 0.7m^3$ volume in front of the robot. Confidence functions **C1** ($R = 0.3m$) and **C2**, were evaluated and the goal configuration was same as in Figure 5 (middle column). Since the target orientations are the same for

Best control dimension distribution				
Confidence Function	X	Y	Z	NULL
C1	579	615	446	360
C2	1711	93	196	0

TABLE I
BEST CONTROL DIMENSION DISTRIBUTION FOR TWO DIFFERENT CONFIDENCE FUNCTIONS.

all goals, disambiguation only happened in the translational dimensions and therefore is reduced to a three-dimensional problem.

Figure 4 shows the results of the simulation. It is clear that the choice of confidence function changes the preferred control dimensions in the workspace quite significantly. Table I also reports the number of times the algorithm picked each of the three control dimensions, for each confidence function.

More importantly, it sheds light on the efficacy of a confidence function in capturing human intent properly. For the goal distribution used in the simulation, the goal positions are spread out maximally along the x and z axes. Intuitively the system will be able to quickly infer the human's intent if the human control command is either along the x or the z axes.

However, under confidence function **C1** the information is equally spread throughout all control dimensions (Table I)—because **C1** contains less information content with respect to intent inference. Furthermore, **C1** had “null” spaces where all confidences were identically equal to zero and therefore disambiguation was not possible.

By contrast, using **C2**, x was identified as the preferred dimension in 1711 out of 2000 samples, and z in 196 of the remaining 289 samples, which indicates that the confidence

n_g	3	4	5
Accuracy%	89.24	87.09	86.11

TABLE II
DISAMBIGUATION ACCURACY FOR OFF-AXIS MOTIONS

function along with our algorithm was able to select the disambiguating dimensions over 95% of the time. The algorithm picked y only when the robot was directly in front of a goal.

B. Characterization of Simplifying Assumption

In our algorithm, the computation of D_m only considers motion projected along perpendicular vectors: the axes of each dimension k_i of mode m . However, in reality the user can generate a control command in any arbitrary direction within the control mode, and so the robot can move along any vector spanned by the control dimensions in m . In order to assess the impact of this simplification, we performed simulations in which m^* was computed for 500 uniformly spaced locations in the robot workspace. At each of those points, 100 random control commands feasible in m^* were generated and applied to perturb the robot. Finally, at each of these perturbed positions the best control mode was once again computed.

If the best mode in the perturbed position was the same mode as m^* , then the simplification did not adversely affect the identification of the disambiguating mode. Table II summarizes the number of times a match occurred for different configurations of the workspace (with $n_g = 3, 4$ and 5). While the simplification holds for 85-90% of off-axis motions, we do observe a trend where performance drops as the number of goals increase. Intuitively this makes sense because disambiguation between goals will become harder as the number of goals increase.

C. Discussion

Our simulation results indicate a strong correlation between the intent inference power of a given confidence function and the disambiguation power of our algorithm. It is unsurprising that confidence functions which are information-poor approximations of human intent also perform less robustly when disambiguating between those approximations. Moreover, the algorithm could be used to pre-compute the most informative modes ahead of time, which then might be called on demand during the task execution—which could prove helpful for complex tasks and/or limited interfaces that require more information from the human for disambiguation.

VI. PILOT STUDY

We next explore the use and utility of our disambiguation approach in a pilot study. Four subjects participated in the pilot study, (3 male, 1 female), and all were lab members.

A. Hardware

The experiments were performed using the MICO robotic arm (Kinova Robotics, Canada), which is a 6 DOF robotic arm specifically designed for assistive purposes. The software

system was implemented using the Robot Operating System (ROS) and data analysis was performed using MATLAB.³

The human control command u_h was captured using two different control interfaces: 2-axis joystick and a head array, shown in Figure 6. For both interfaces, the control interface signals are mapped to Cartesian velocities of the end effector of the robot. Additionally, the interfaces can also be used to request mode switch assistance. In using two interfaces, we hope to observe an increase in task effort for the head array due to the limited bandwidth and discrete nature of the signals.

In detail, the 2-axis joystick generates continuous signals and is capable of controlling a maximum of two control dimensions at a time. Different control modes can be accessed using the buttons on the interface. The head array generates 1-D discrete control signals, and consists of three switches operated by the head and embedded within the back and sides of the headrest. When used for controlling a robotic arm, the switch at the back is used to cycle between the control modes, and the switches on the left and right side control the motion of the end-effector in the positive and negative direction along a control dimension of the selected control mode.



Mode	Head Array	Joystick
1	v_x	v_x, v_y
2	v_y	v_x, v_z
3	v_z	ω_x, ω_y
4	ω_z	ω_x
5	ω_y	—
6	ω_x	—

Fig. 6. A 2-axis joystick (left) and switch-based head array (center) and their operational paradigms (right). v and ω indicate the translational and rotational velocities of the end effector respectively.

B. Assistance Paradigms

Three kinds of mode switching paradigms were evaluated. Note that the blending assistance (as described in Section IV-B) was always running for all three paradigms. Since under the blending paradigm the amount of assistance directly depends on the amount of confidence, this means that if the intent inference improves as a result of disambiguation, more assistance will be provided by the robot.

Manual: The trial starts in a randomized initial mode and during task execution the user manually performs all subsequent mode switches.

Disambiguation: The disambiguation system is activated right at the beginning of a trial. The algorithm identifies the “best mode” m^* and starts the trial in mode m^* . All subsequent mode switches are performed manually by the user. Furthermore, the user is required to first move in the selected mode before manually switching the mode.

On Demand: The user can request mode switch assistance at any time during the task execution. This paradigm is

³Additionally, for the 6-D robot arm implementation, the computation of $C2$ is split into translational and rotational component. (In Section V, only translational components were considered). Here confidence function $C2$ is computed as $c(x, u_h, u_{r,g}) = u_h^{trans} \cdot (x_g - x)^{trans} + u_h^{rot} \cdot u_{r,g}^{(rot)}$ where *trans* refers to the translational and *rot* refers to the rotational parts of the entire control space.

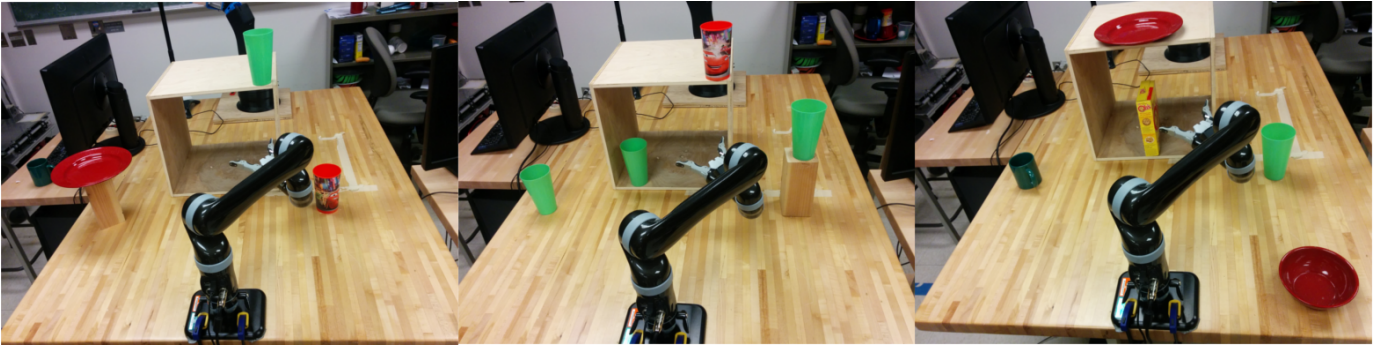


Fig. 5. Pilot study tasks. Left to right: Training, Testing (Easy), Testing (Hard).

exploratory and seeks to find underlying patterns in assistance request behavior.

C. Tasks, Metrics and Protocol

Tasks: Tasks developed for our pilot study consisted of the following (Figure 5). **Training:** The user operates the robotic arm to perform simple reaching motions to three different goal locations. This is a training task and the primary purpose is to get the user accustomed to the operation of the interfaces, the blending-based assistance and the experiment protocol. **Testing:** The user operates the robotic arm under two scenarios of varying difficulty. *Easy:* Four objects, all with the same grasp orientations. *Hard:* Five objects, all with different grasp orientations.

Metrics: *Task completion time* is the amount of time a user spends in accomplishing a task. *Mode switches* refer to the number of times the user switched between various modes while performing the task and is an indicator of effort.

Protocol: A within-subject study was conducted using a full factorial design in which the manipulated variables are the tasks, control interfaces and assistance paradigms. Each task consisted of two phases.

In Phase I, each user performed the task using both interfaces under *Manual* and *Disambiguation* paradigms. The trials were balanced and the control interfaces and the paradigms were randomized to eliminate ordering effects. The starting positions of the robot were also randomized to avoid biases. Three trials were collected for each permutation of manipulated variables. In Phase II, the user performed the same task using both interfaces using the *on-demand* paradigm and two trials were collected for each task-interface combination.

D. Pilot Study Results

An improvement in task performance in terms of a decrease in the number of mode switches was observed across both interfaces. Statistical significance in Figure 7 is determined by two-sided Wilcoxon Rank-Sum Test, where (*) indicates $p < 0.05$ and (***) indicates $p < 0.001$.

Mode Switches: Figure 7 (top row) reveals a general trend of a decrease in the number of mode switches when disambiguation

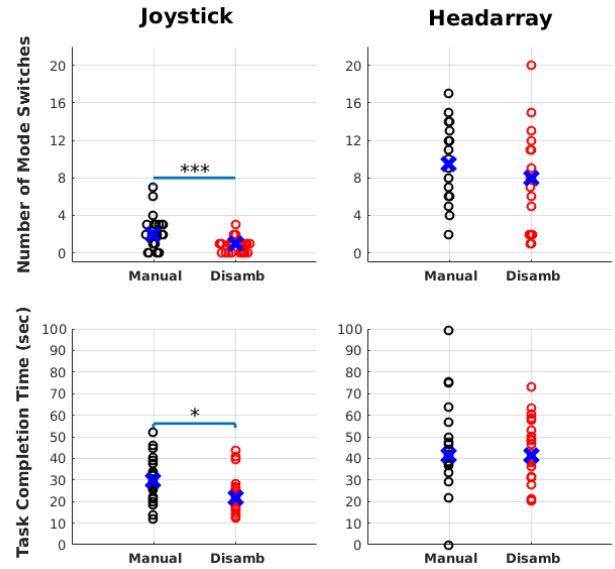


Fig. 7. Comparison of Disambiguation and Manual paradigms. Operation using joystick (left column) and head array (right column) interfaces. Evaluation of mode switches (top row) and completion time (bottom row). \times indicates the median.

assistance is employed. However, the difference was statistically significant only when using the joystick. This indicates that upon starting in a mode identified by the algorithm, the number of subsequent mode switches performed by the user was reduced.

Task Completion Time: In Figure 7 (bottom row), a statistically significant decrease in task completion times between the *Manual* and *Disambiguation* paradigms was observed when using the joystick. The task completion times were comparable between the two paradigms when using the head array. This can be possibly explained by the fact that a *single* mode switch assistance at the beginning of the trial probably did not have a measurable impact in reducing the subsequent number of mode switches needed when using a head array which requires many more mode switches to achieve a task—as seen in the top row of Figure 7.

On-Demand: The number of disambiguation requests under

SubID	Joystick		Head Array	
	Easy	Hard	Easy	Hard
H1	1	0	5	6
H2	1	1	3	6
H3	2	2	4	5
H4	2	5	17	7

TABLE III
NUMBER OF DISAMBIGUATION REQUESTS

the on-demand paradigm are reported in Table III. Although the subjects demonstrated a wide range of disambiguation request behaviors, we were able to observe a general trend of an increase in disambiguation requests with an increase in task difficulty. This shows that users were keen to explore the *on-demand* option when the tasks became more difficult.

E. Future Work

Post-experiment feedback from the users also revealed that the subjects found the disambiguation assistance to be counter-intuitive at times in the on-demand paradigm. This can be attributed to two main limitations of the current algorithm.

Currently when the user requests assistance (in the on-demand paradigm) at any point in time and space, the algorithm discards all information contained in the history of user commands from the start of the trial until that point. That is, the disambiguation algorithm lacks *memory* and reasons about the user's intent solely based on information that is available locally (in time and space). However, it might be useful to bias the computation of the disambiguating control mode by incorporating information from the past history of the robot trajectory and control commands by having a non-uniform prior over the intended goals. This will also likely improve the robustness, efficacy of the algorithm and result in higher user acceptance.

Secondly, the algorithm only tries to maximize the utility value for the robot (as encoded in the disambiguation metric D_m). It is also important to take into account the users' preferences and utility for operating in the mode selected by the algorithm. Concepts from decision theory and expected utility theory can be used to enhance the current framework.

Our pilot study revealed some promising trends and therefore a more extensive user study with motor-impaired subjects will be conducted in the future to evaluate the utility value of the disambiguation assistance system and further explore and understand the disambiguation request patterns of users.

VII. CONCLUSIONS

In this paper, we have presented an algorithm for *intent disambiguation assistance* with a shared-control robotic arm. We also introduced the notion of *inverse legibility*, in which the human-generated actions are legible enough for the robot to infer the human intent confidently and accurately. The goal of the algorithm developed in this paper is to seek legible control commands from the human by placing the control in those

modes able to *maximally disambiguate* between the various goals in the scene. Preliminary pilot study results suggest that the disambiguation paradigm proposed in this work to be promising. Our simulation work evaluated the robustness of the algorithm and the impact of different confidence functions on intent disambiguation. In our future work, as informed by the pilot study we plan to enhance our algorithm, to improve task performance and extend the framework into an automated mode switch assistance system.

ACKNOWLEDGMENTS

This material is based upon work supported by the National Science Foundation under Grant CNS 15544741. Any opinions, findings and conclusions or recommendations expressed in this material are those of the authors and do not necessarily reflect the views of the aforementioned institutions.

REFERENCES

- [1] Nikolay Atanasov, Jerome Le Ny, Kostas Daniilidis, and George J. Pappas. Information acquisition with sensing robots: Algorithms and error bounds. In *IEEE International Conference on Robotics and Automation (ICRA)*, 2014.
- [2] Chris L. Baker, Joshua B. Tenenbaum, and Rebecca R. Saxe. Goal inference as inverse planning. In *Proceedings of the Cognitive Science Society*, 2007.
- [3] Chris L. Baker, Rebecca R. Saxe, and Joshua B. Tenenbaum. Action understanding as inverse planning. *Cognition*, 113(3):329–349, 2009.
- [4] Chris L. Baker, Julian Jara-Ettinger, Rebecca R. Saxe, and Joshua B. Tenenbaum. Rational quantitative attribution of beliefs, desires and percepts in human mentalizing. *Nature Human Behaviour*, 1:0064, 2017.
- [5] Clark H. Barrett, Peter M. Todd, Geoffrey F. Miller, and Philip W. Blythe. Accurate judgments of intention from motion cues alone: A cross-cultural study. *Evolution and Human Behavior*, 26(4):313–331, 2005.
- [6] Young Sang Choi, Cressel D. Anderson, Jonathan D. Glass, and Charles C. Kemp. Laser pointers and a touch screen: intuitive interfaces for autonomous mobile manipulation for the motor impaired. In *Proceedings of the International SIGACCESS Conference on Computers and Accessibility*, 2008.
- [7] John P. Donoghue. Connecting cortex to machines: recent advances in brain interfaces. *Nature Neuroscience*, 5: 1085–1088, 2002.
- [8] Anca D. Dragan and Siddhartha S. Srinivasa. Assistive teleoperation for manipulation tasks. In *Proceedings of ACM/IEEE International Conference on Human-Robot Interaction (HRI)*, 2012.
- [9] Anca D. Dragan and Siddhartha S. Srinivasa. *Formalizing assistive teleoperation*. MIT Press, 2012.
- [10] Anca D. Dragan and Siddhartha S. Srinivasa. A policy-blending formalism for shared control. *The International Journal of Robotics Research*, 32(7):790–805, 2013.

- [11] Anca D. Dragan, Kenton CT. Lee, and Siddhartha S. Srinivasa. Legibility and predictability of robot motion. In *Proceedings of the ACM/IEEE International Conference on Human-Robot Interaction (HRI)*, 2013.
- [12] Ian J. Goodfellow, Nate Koenig, Marius Muja, Caroline Pantofaru, Alexander Sorokin, and Leila Takayama. Help me help you: Interfaces for personal robots. In *Proceedings of ACM/IEEE International Conference on Human-Robot Interaction (HRI)*, 2010.
- [13] Deepak Gopinath, Siddarth Jain, and Brenna D. Argall. Human-in-the-loop optimization of shared autonomy in assistive robotics. *IEEE Robotics and Automation Letters*, 2(1):247–254, 2017.
- [14] Laura V. Herlant, Rachel M. Holladay, and Siddhartha S. Srinivasa. Assistive teleoperation of robot arms via automatic time-optimal mode switching. In *Proceedings of the ACM/IEEE International Conference on Human-Robot Interaction (HRI)*, 2016.
- [15] Rachel M. Holladay, Anca D. Dragan, and Siddhartha S. Srinivasa. Legible robot pointing. In *The IEEE International Symposium on Robot and Human Interactive Communication (RO-MAN)*, 2014.
- [16] Lauren M. Miller and Todd D. Murphey. Trajectory optimization for continuous ergodic exploration. In *American Control Conference (ACC)*, 2013.
- [17] Lauren M. Miller, Yonatan Silverman, Malcolm A. MacIver, and Todd D. Murphey. Ergodic exploration of distributed information. *IEEE Transactions on Robotics*, 32(1):36–52, 2016.
- [18] Stephen Monsell. Task switching. *Trends in cognitive sciences*, 7(3):134–140, 2003.
- [19] Marnix Nuttin, Dirk Vanhooydonck, Eric Demeester, and Hendrik Van Brussel. Selection of suitable human-robot interaction techniques for intelligent wheelchairs. In *Proceedings of the IEEE International Workshop on Robot and Human Interactive Communication*, 2002.
- [20] Stephanie Rosenthal, Joydeep Biswas, and Manuela Veloso. An effective personal mobile robot agent through symbiotic human-robot interaction. In *Proceedings of the International Conference on Autonomous Agents and Multiagent Systems*, 2010.
- [21] Alexander Sorokin, Dmitry Berenson, Siddhartha S. Srinivasa, and Martial Hebert. People helping robots helping people: Crowdsourcing for grasping novel objects. In *IEEE/RSJ International Conference on Intelligent Robots and Systems (IROS)*, 2010.
- [22] Katherine Tsui, Holly Yanco, David Kontak, and Linda Beliveau. Development and evaluation of a flexible interface for a wheelchair mounted robotic arm. In *Proceedings of the ACM/IEEE International Conference on Human-Robot Interaction (HRI)*, 2008.
- [23] Ivan Volosyak, Oleg Ivlev, and Axel Graser. Rehabilitation robot FRIEND II-the general concept and current implementation. In *Proceedings of the International Conference on Rehabilitation Robotics (ICORR)*, 2005.